

# Finite Element Analysis of Warp of Diamond Wire-cut Monocrystalline Silicon Slices

Xiaokang Liu\*

Tianjin Key Lab of High Speed Machining & Precision Machining, Tianjin University of Technology and Education, Tianjin 300222, China

\*Corresponding author Email: lxk040510@163.com

---

## Abstract

The warp of monocrystalline silicon slices seriously affects the surface quality of the slices, which is a quality factor that must be controlled during the cutting process. By establishing a thermodynamically coupled finite element analysis model for single-wire cutting of monocrystalline silicon, the warp of the slice is simulated using the nodal displacement of the slice surface. Firstly, a temperature field finite element model is established to simulate the temperature field distribution on the slices under different line speeds, feed speeds, tensions, wire diameters, and applied temperature loads; after that, the thermal deformation of the slices is simulated and analysed with the results of the temperature field as the boundary conditions, and the values of the warp of the slices are calculated, and the relationship between slices' warp and the temperature field is studied. The results show that the larger the line speed and feed speed are, the more obvious the warp deformation is; the larger the tension and line diameter are, the smaller the warp deformation is. The warp deformation of the slices is more obvious after the external temperature load is applied.

## Keywords

Monocrystalline Silicon; Diamond Wire Cutting; Cutting Temperature; Warp; Finite Element Analysis.

---

## 1. Introduction

Semiconductor materials are widely used in various important fields such as electronic information, energy, communication, military and aerospace and aviation due to their unique properties such as electrical conductivity, photosensitivity and thermal sensitivity [1]. Compared with other semiconductor materials, monocrystalline silicon has stable performance, high purification precision, and low manufacturing cost, which makes it an important basic material for large-scale integrated circuits, solar photovoltaics, electronic devices, and other fields, especially in the integrated circuit industry, which accounts for more than 90% of the total [2]. At present, integrated circuits are becoming more and more integrated, the number of wiring layers is increasing, and the size of the components used is getting smaller and smaller [3]. Therefore, the substrate wafers used in the IC industry at this stage need to meet the high-quality requirements such as high surface flatness of the slices, shallow damage layer, and small roughness. Take the 300 mm monocrystalline silicon wafer substrate which is widely used at present as an example, it is required to have a purity of 99.99999999999999%, a total thickness variation of no more than 0.3 $\mu$ m, a flatness of less than 40 nm, no obvious damage to the surface and subsurface, and a high degree of strength [4]. In order to meet these requirements, monocrystalline silicon wafers are developing towards large size, thin thickness and high quality. However, with the increasing size of the wafer, the wafer is highly susceptible to

warp deformation, and among the many performance parameters of the wafer, the warp has the most serious impact on the surface quality of the wafer. Dicing is a key step in the production of substrate wafers, accounting for 40% of the total production cost, and it is also the step in which wafers are most susceptible to warp deformation [5].

Diamond wire cutting technology has the advantages of good slice quality, small loss of saw slit, low cost, and environmental friendliness, and has become the mainstream way of monocrystalline silicon cutting at this stage [6]. It mainly uses the chemical plating method, resin bonding method or brazing method to fix the diamond abrasive grains on the surface of the steel wire, and in the cutting process, the steel wire carries out high-speed movement under the drive of the guide wheel, and the diamond abrasive grains cemented on the surface of the steel wire grind and scrape with the same speed in the cutting area until the cutting is completed [7]. In the cutting process, the diamond particles continuously grind the silicon ingot, and the energy consumed is almost completely converted into heat, and it is found by related scholars that 1/2 to 1/3 of the heat generated is absorbed by the silicon ingot, the temperature of the cutting area rises while the temperature of the non-cutting area stays unchanged, and the slices are warped and deformed under the effect of thermal expansion and cold contraction. It was shown that when cutting and processing 200 mm silicon rods, the temperature in the cutting region increased by 20°C and the thermal deformation of the slices was 10.4 μm [8]. Therefore, the study of the relationship between the temperature distribution during the cutting process and the warp deformation of the slices is of great practical significance for improving the surface quality of the slices and promoting industrial production.

## 2. Thermodynamic Analysis Model

The study of thermodynamic problems in diamond wire cutting single crystal silicon process mainly includes two aspects: heat transfer problem, used to determine the temperature field distribution on the slices in the cutting process; thermal stress problem, used to determine the stress-strain distribution of the slices after cutting. Combined with the diamond wire cutting single crystal silicon, the temperature field directly affects the stress-strain field, while the thermal stress field for the temperature field can be almost ignored, so this paper uses Abaqus sequential thermal coupling analysis method to simulate the cutting process.

### 2.1 Heat Transfer Modelling for Wire Cutting

Monocrystalline silicon cutting belongs to the high-speed cutting process, in processing, based on the energy conservation theorem and Fourier's law of heat transfer, can be established in the cutting process of the control equation of heat transfer, that is, the transient temperature field  $T(x, y, z, t)$  of the silicon ingot cutting needs to satisfy the following equation:

$$\frac{\partial}{\partial x} \left( K_x \frac{\partial T}{\partial x} \right) + \frac{\partial}{\partial y} \left( K_y \frac{\partial T}{\partial y} \right) + \frac{\partial}{\partial z} \left( K_z \frac{\partial T}{\partial z} \right) + q = \rho C_p \frac{\partial T}{\partial t} \quad (1)$$

Where:  $\rho$  is the density of the material in kg/m<sup>3</sup>,  $C_p$  is the specific heat capacity of the material in J/(kg·k).  $k(x,y,z)$  is the heat transfer coefficient along the x,y,z direction in W/(m·K).  $q$  is the density of the heat flow in W/m<sup>2</sup>.  $t$  is the time for which the process is carried out in s.

Heat flow density is the amount of heat that passes through an object per unit of cross-sectional area per unit of time. For sawing process the heat flow density can be understood as the power applied per unit sawing area [9]. For wire saw cutting simulation, it is usually loaded on the contact semicircle of the cutting kerf.

The heat flow density is calculated by the formula:

$$q = \varepsilon \frac{\mu P}{S} \quad (2)$$

Where:  $\varepsilon$  is the coefficient of cutting heat transfer to the surface of the crystal rod, related to the contact length of the wire saw and the crystal as well as the wire bow angle of the diamond wire, and is a dimensionless quantity. It can be expressed as:

$$\varepsilon = L \sin \alpha \quad (3)$$

Where: L is the contact length between the wire saw and the crystal;  $\alpha$  is the wire bow angle for diamond wire cutting.

$\mu$  is the coefficient of heat generated in the cutting process removed by the coolant to be taken away and absorbed by the crystals, it is found that 1/2~2/3 of the cutting heat generated is absorbed by the workpiece, and in this paper, the heat absorption coefficient  $\varepsilon$  is taken as 0.66;

P is the wire saw cutting power, which can be expressed as the product of diamond wire tension and wire speed, as shown in the following equation:

$$P = FV_s \quad (4)$$

Where: F is the tension of the wire saw;  $V_s$  is the linear velocity;

S is the cross-sectional area of the cut, which can be expressed as the product of the contact length and the diamond wire diameter, as shown in the following equation:

$$S = Ld \quad (5)$$

Where: d is the width of the cutting saw kerf;

Therefore, the heat flow density in sawing process can be obtained by combining the above equations:

$$q = \mu \frac{FV_s}{d} \sin \alpha = \mu \frac{LFV_s V_f t}{A} \sin \alpha \quad (6)$$

Where:  $V_f$  is the feed speed, A is the volume of material removed per analysis step, and t is the time per analysis step;

## 2.2 Models for Thermal Strain Analysis

Monocrystalline silicon is a typical hard and brittle material, and this paper does not consider its plasticity when carrying out the research, and adopts the basic theory of thermoelastic mechanics to analyse it. When the temperature distribution inside the object is uneven, it will lead to thermal expansion and contraction of the components and generate thermal stresses, according to the linear thermodynamics theory, the total strain of the microelement inside the object consists of two parts: the strain caused by the temperature change and the strain caused by the stress [10]. The strain induced by the temperature difference is  $\varepsilon_{ij}^f = [\alpha] \Delta T$ , after which the structure is discretised for the variational component, the relation between the unit nodal force and nodal displacement can be obtained as:

$$K^e q^e = p^e + p_f^e \quad (7)$$

Where:  $p_f^e$  is the temperature equivalent load.

### 3. Finite Element Modelling

Abaqus simulation software is used to simulate the cutting process of monocrystalline silicon. The size of the monocrystalline silicon ingot is 85×90×1.25 mm, and the width of the saw slit is taken as the width of the diamond wire diameter, which is 0.25 mm. The mesh division is encrypted for the saw slit part of the mesh, and the mesh division is shown in Fig.1. The physical parameters of monocrystalline silicon are shown in Table 1 below [11].

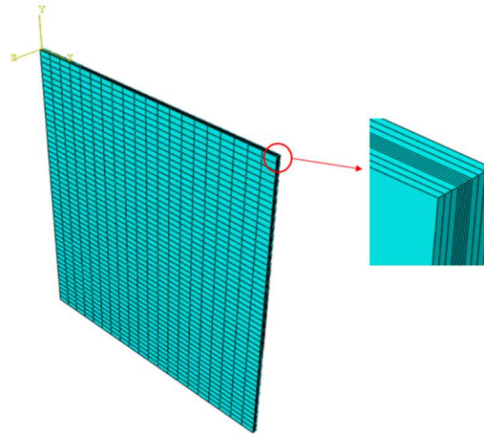


**Fig. 1** Finite element model of saw-cut single crystal silicon

**Table 1.** physical parameter of monocrystalline silicon

physical parameter	numerical value
densities( $T/mm^3$ )	$2.339 \cdot 10^{-9}$
Young's modulus(MPa )	$1.9 \cdot 10^{-5}$
Poisson's ratio	0.28
heat conductivity(MW/mm/°C)	150
Coefficient of thermal expansion(°C <sup>-1</sup> )	$2.6 \cdot 10^{-6}$
specific heat capacity(mJ/T/°C)	$7 \cdot 10^8$

To carry out the simulation, the removal of material is modelled using a birth-death unit algorithm, and the movement of the heat source is simulated by the application of dynamic load steps. It is shown that for natural convection, the heat transfer coefficient of air is generally in the range of 1 to 10 W/m<sup>2</sup>/°C, and the heat transfer coefficient of water is generally in the range of 200 to 1000 W/m<sup>2</sup>/°C. In this paper, the heat transfer coefficient is taken to be 0.05 W/m<sup>2</sup>/°C in order to better compare the temperature changes in each area on the slices during the cutting and processing stage.

### 4. Finite Element Result Analysis

Warp is the difference between the maximum and minimum distance between the middle of the slice and an imaginary reference plane when the slice is not subjected to an external force. Warp is a more comprehensive response to slice deformation than Bow.

In the finite element simulation, the thermal deformation displacement of the nodes on the wafer surface is used to indirectly reflect the warp of the wafer [12]. To calculate the warp, the corresponding nodes on the wafer surface perpendicular to the direction of wire travelling are selected and their displacement values are read, and the difference between the maximum displacement value and the minimum displacement value is the warp value of the wafer, as shown in Fig.2.

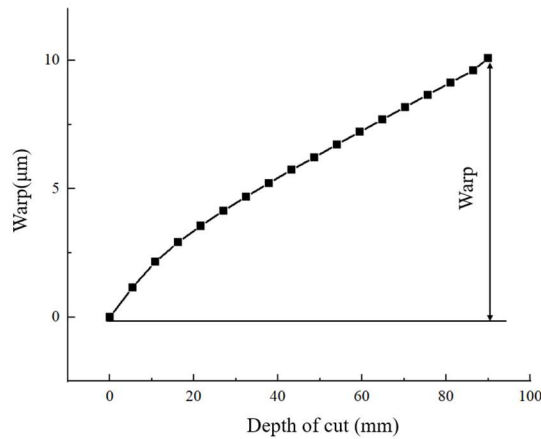


**Fig. 2** Calculation method of slice warp

#### 4.1 Effect of Line Speed on Warp

When the feed speed is 0.2 mm/min, the tension force is 30 N, and the wire diameter of the diamond wire is 0.25 mm, the size of the wire speed is changed to analyse the relationship between the wire speed and the warp of the slices, and the results are shown in Fig. 5. The results are shown in Fig.3. It can be seen that the relationship between the wire speed and the warp of the slices is directly proportional to each other, and the warp of the slices is 1.888, 2.349, 2.818, and 3.287 $\mu\text{m}$  when the wire speed is 4, 5, 6, and 7 m/s. The increase of the wire speed from 4 to 7 m/s increases the warp of the slices by 74.4%. Selecting a smaller wire speed for cutting can effectively reduce the warp of the slices, but too small a wire speed will affect the cutting ability of the diamond wire.

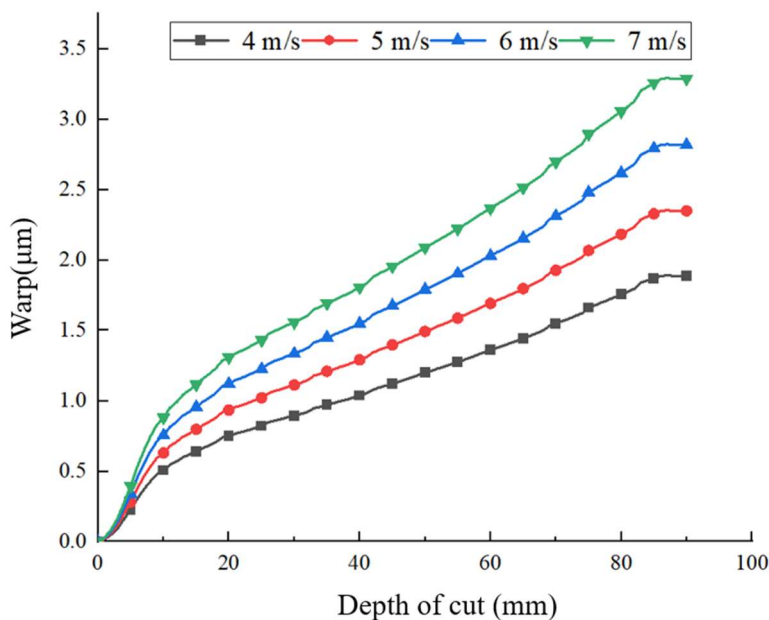


**Fig. 3** Relationship between wire speed and warp

#### 4.2 Effect of Feed Speed on Slice Warp

When the wire speed is 4 m/s, the tension force is 30 N, and the wire diameter of diamond wire is 0.25 mm, the size of the feed speed is changed to analyse the relationship between the feed speed and the warp of the slices, and the results are shown in Fig. 6. The results are shown in Fig.4. It can be seen that the feed speed is proportional to the warp of the slices, and the warp of the slices is 1.247, 1.888, 2.504, and 3.133 $\mu\text{m}$  for the feed speeds of 0.2, 0.3, 0.4, and 0.5 mm/min, respectively, and the warp of the slices is 151.2% for the feed speed of 0.2 mm/min and 0.5mm/min, respectively. 151.2%.

Selecting a smaller feed speed for cutting can effectively reduce the warp of the slices, but too small a feed speed will affect the cutting efficiency.

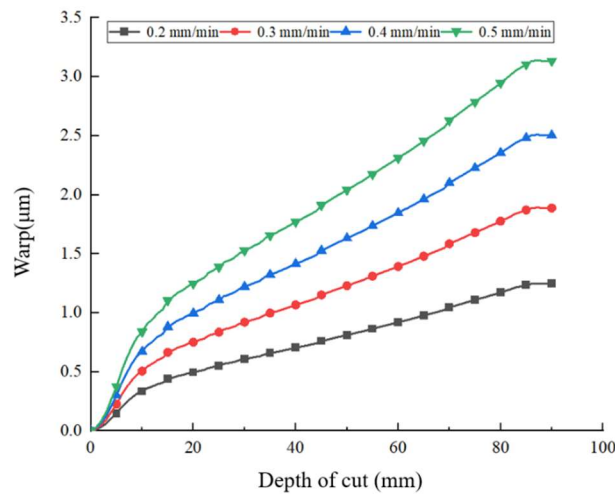


Fig. 4 Relationship between feed speed and warp

#### 4.3 Effect of Tension on Slice Warp

When the wire speed is 4 m/s, the feed speed is 0.2 mm/min, and the wire diameter of the diamond wire is 0.25 mm, the size of the tension force is changed to analyse the relationship between the tension force and the warp of the slices, and the results are shown in Fig.5. The results are shown in Fig. 7. It can be seen that the tension force is inversely proportional to the warp of the slices, and the warp of the slices is 2.106, 1.888, 1.432, and 0.8389 $\mu\text{m}$  for the tension forces of 25, 30, 35, and 40 N. The increase of the tension force from 25 N to 40 N reduces the warp of the slices by 60.2%. The warp of the slices can be effectively reduced by choosing a higher tension force for cutting, but the tension force is too high to increase the risk of diamond wire breakage.

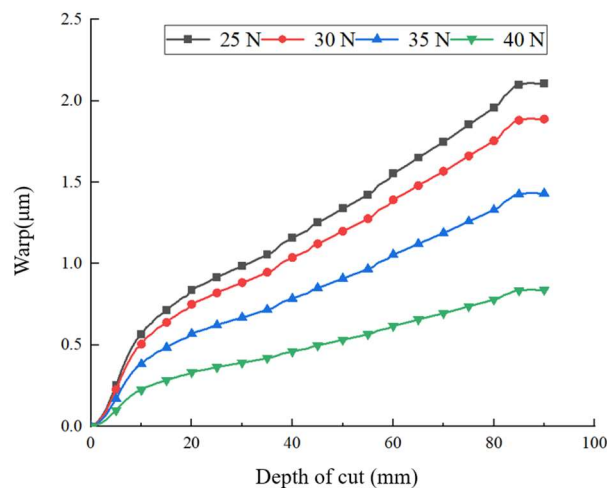


Fig. 5 Relationship between tension and warp

#### 4.4 Influence of Wire Diameter on the Warp of Slices

When the wire speed is 4 m/s, the feed speed is 0.2 mm/min and the tension force is 30 N, the size of the wire diameter is varied to analyse the relationship between the wire diameter and the warp of the slices, and the results are shown in Fig. 8. The results are shown in Fig.6. From the figure, it can be seen that there is an inverse relationship between the wire diameter and the warp of the slices, and the warp of the slices is 1.888, 1.678, 1.566, and 1.343 $\mu\text{m}$  for the wire diameters of 0.25 mm, 0.28, 0.30, 0.35 mm, respectively, and the warp of the slices decreases by 28.9% when the wire diameter

is increased from 0.25 mm to 0.35 mm. The warp of the slices can be effectively reduced by choosing diamond wires with larger wire diameters for cutting, but too large a wire diameter will result in an increase in the loss of saw kerf and a decrease in the slice yield.

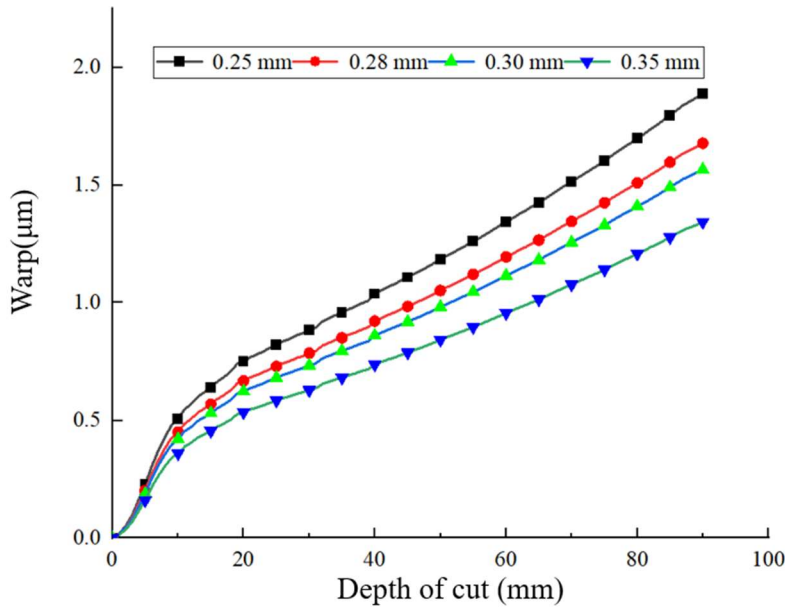


Fig. 6 Relationship between wire diameter and warp

#### 4.5 Effect of Applied Temperature Load on the Warp of Slices

When the wire speed is 4 m/s, the feed speed is 0.2 mm/min, the tension force is 30 N, and the diameter of the wire is 0.25 mm, the temperature load is applied to the left and right sides of the silicon ingot to analyse the relationship between the temperature load and the warp of the slices, and the results are shown in Fig.7. From Fig. 9, it can be seen that the thermal deformation of the slices gradually increases with the increasing of the sawing depth, and according to the calculation method of the slice warp in the finite element analysis, the slice warp can be obtained as 10.09µm.

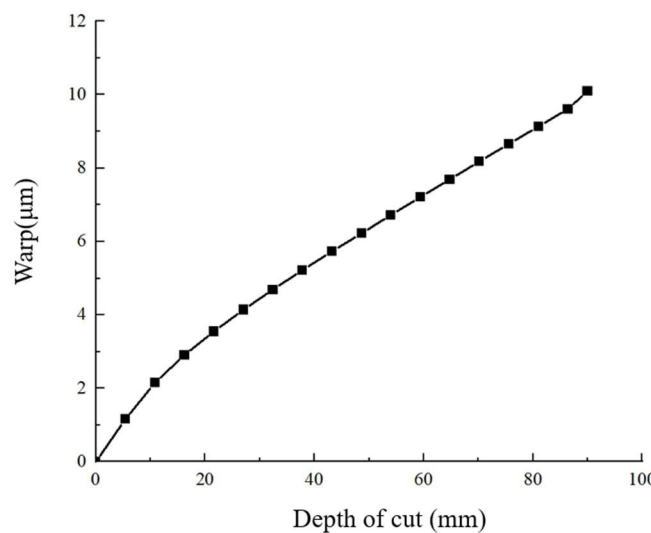


Fig. 7 Warp deformation of slices after applying temperature loads

### 5. Conclusion

In this paper, by establishing a finite element model for the sequential coupled heat-strain analysis of diamond wire sawing single crystal silicon, the warp deformation of the slice is reflected by the nodal

displacement of the slice surface. The warp deformation of the slices under different wire speed, feed speed, tension, wire diameter and external heating load is studied, and the results show that: the warp of the slices is positively correlated with the wire speed and feed speed, and negatively correlated with the tension and wire diameter, and the warp deformation of the slices is more significant after the external heating load. In the actual production and processing, the process parameters should be selected reasonably, and a smaller wire speed and feed speed and a larger tension should be selected under the permitted circumstances, which is conducive to obtaining high-quality slices.

## References

- [1] Bhagavat S, Kao I. Ultra-low load multiple indentation response of materials: In purview of wire saw slicing and other free abrasive machining (FAM) processes[J]. *International Journal of Machine Tools and Manufacture*, 2007, 47(3-4): 666-672.
- [2] Kang RK, Tian YB, Guo DM, et al. Current status of research and application of ultra-precision grinding technology for large-diameter silicon wafers[J]. *Diamond and Abrasives Engineering*, 2003, (04):13-18+25.
- [3] Jung M, Mitra J, Pan D Z, et al. TSV stress-aware full-chip mechanical reliability analysis and optimization for 3D IC[J]. *Communications of the ACM*, 2014, 57(1): 107-115.
- [4] Ge PQ, Chen ZB, Wang PZ, et al. Research progress of processing technology of monocrystalline silicon slices[J]. *Diamond and abrasives engineering*, 2020, 40(04):12-18.
- [5] Li Y, Wang XH, Li SJ, et al. Experimental study of ultrasound-assisted wire saw cutting of SiC single crystals[J]. *Journal of Artificial Crystals*, 2012, 41(04):1076-1081.
- [6] Zhang FL, Yuan H, Zhou YM, et al. Research Progress of Multi-Wire Saw for Precision Cutting of Silicon Wafers[J]. *Diamond and Abrasives Engineering*, 2006, (06):14-18.
- [7] Zeng M, Zhou YM, Guo CW, et al. Advances in Solid Abrasive Multi-Wire Saw Research [J]. *Superhard Materials Engineering*, 2007(05):1-5.
- [8] Bhagavat S, Kao I. A finite element analysis of temperature variation in silicon wafers during wiresaw slicing[J]. *International Journal of Machine Tools and Manufacture*, 2008, 48(1): 95-106.
- [9] Jiao Y. Coupled analysis of the sawing stress field in KDP crystal solidified abrasive grain wire saws [D]. Shandong University, 2014.
- [10] Chen Y. Finite element analysis of microcrack damage depth and warp in SiC single crystal wire saw slices [D]. Shandong University, 2017.
- [11] Chen DM. Finite element analysis of stress field in diamond wire saw slicing processing of photovoltaic polysilicon [D]. Shandong University, 2022.
- [12] Yamada T, Kinai F, Ichikawa T, et al. Warp Analysis of Silicon Wafer in Ingot Slicing by Wire-Saw Machine[C]//AIP Conference Proceedings. American Institute of Physics, 2004, 712(1): 1459-1463.